

**Many-body theory of carrier capture and relaxation in semiconductor quantum-dot lasers**T. R. Nielsen,<sup>1</sup> P. Gartner,<sup>1,2</sup> and F. Jahnke<sup>1,\*</sup><sup>1</sup>*Institute for Theoretical Physics, University of Bremen, D-28334 Bremen, Germany*<sup>2</sup>*National Institute for Materials Physics, POB MG-7, Bucharest-Magurele, Romania*

(Received 1 October 2003; revised manuscript received 23 February 2004; published 21 June 2004)

In quantum-dot laser devices containing a quasi-two-dimensional wetting layer, a pump process initially populates the wetting-layer states. The scattering of carriers from these spatially-extended quasi-two-dimensional states into the quantum-dot states as well as the relaxation of carriers between the quantum-dot levels are studied theoretically. Based on the wave functions for the coupled quantum-dot/wetting-layer system interaction matrix elements are calculated for carrier-carrier Coulomb interaction and carrier-phonon interaction. Scattering rates for various capture and relaxation processes are evaluated under quasiequilibrium conditions. For elevated carrier densities in the wetting layer, Coulomb scattering provides processes with capture (relaxation) times typically faster than 10 ps (1 ps). When energy conservation allows for interaction with LO phonons, comparable rates are obtained.

DOI: 10.1103/PhysRevB.69.235314

PACS number(s): 73.21.La, 78.67.Hc

**I. INTRODUCTION**

To optimize the design of novel quantum-dot (QD) based laser devices<sup>1,2</sup> as well as to provide a detailed understanding of steady-state and dynamical emission properties in these devices,<sup>3,4</sup> a quantitative description of various electronic scattering processes is necessary. Self-assembled QD's are typically grown on a quasi-two-dimensional wetting layer (WL). Correspondingly, the relevant electronic structure consists of two parts. The localized QD states with discrete energies due to the three-dimensional QD confinement potential are energetically below a quasicontinuum of two-dimensional delocalized WL states. While the localized QD states are used for the laser transition, the pump process initially generates carriers in the WL. Hence the carrier dynamics in QD based laser devices critically depends on the capture of carriers from the WL into the QD's as well as on the relaxation of carriers between the discrete QD states. An important question is to what extent these processes limit the laser operation in comparison to the extensively studied quantum-well lasers.<sup>5</sup>

In laser devices the pump process creates a high density electron-hole plasma in the delocalized states. Under these conditions carrier-carrier scattering can provide efficient transitions for electrons and holes from the delocalized WL states into the discrete localized QD states (carrier capture) as well as between the discrete QD states (carrier relaxation).<sup>6,7</sup> In previous references the transition rates have been calculated for processes where an electron or hole is scattered from the WL into the QD or between two QD states and the energy is transferred to another carrier in the WL. A detailed inspection of the kinetic equation for Coulomb scattering shows that these are only some of the possible processes. A relaxation process starting with two carriers in an excited QD state where one is scattered into the QD ground state and the other into the WL, studied in Ref. 8, is only one among other examples. The analysis in Ref. 6 has been simplified by assuming QD states of a three-dimensional infinite-barrier box. More realistic wave functions for this calculation have been used in Ref. 9 and the dependence of

scattering rates on the QD geometry has been studied in Ref. 10.

On the other hand, interaction with LO-phonons can also lead to efficient scattering channels provided that energy conservation can be fulfilled. While the energy separation of QD states typically does not match the LO-phonon energy, capture processes of carriers from the WL to the QD states are often possible for holes since they have a shallower confinement energy than electrons. In Refs. 11 and 12 capture rates have been computed using Fermi's golden rule, i.e., population effects are neglected.

Experimental evidence for fast capture and relaxation processes is given by the strong QD ground-state photoluminescence following an excitation of the WL or barrier states. From the rise time of the QD photoluminescence<sup>13,14</sup> and the ratio of the QD and WL emission<sup>15</sup> the efficiency of capture and relaxation at low temperatures has been studied. Also it has been pointed out that it is not the two-dimensional nature of the WL but the availability of a quasicontinuum of states that facilitates the scattering processes.<sup>16</sup>

The aim of this paper is to present a systematic study of the relative importance of various capture and relaxation processes due to carrier-carrier and carrier-LO phonon scattering. Previous investigations are extended in the following directions: (i) calculations are not restricted to Fermi's golden rule but include population effects, (ii) both in- and out-scattering processes are considered for the calculation of capture and relaxation times, (iii) additional scattering processes and the role of Coulomb exchange contributions to the scattering integrals are examined, (iv) properly orthogonalized states are systematically used and the influence of the wave function model on the scattering rates is analyzed, and (v) a theoretical model of screening in the coupled QD-WL system is provided.

**II. THEORY FOR COULOMB SCATTERING****A. Boltzmann's equation**

The carrier dynamics under the influence of various scattering processes can be described by kinetic equations. In

this section we consider Coulomb-interaction processes up to quadratic order in the screened Coulomb potential (second-order Born approximation) and restrict ourselves to time scales where the Markov approximation is valid. On this level, the changes of the carrier population  $f_\nu$  in the state with energy  $\varepsilon_\nu$  due to carrier-carrier scattering are given by

$$\begin{aligned} \frac{\partial}{\partial t} f_\nu &= \frac{2\pi}{\hbar} \sum_{\nu_1, \nu_2, \nu_3} W_{\nu\nu_2\nu_3\nu_1} [W_{\nu\nu_2\nu_3\nu_1}^* - W_{\nu\nu_2\nu_1\nu_3}^*] \\ &\times \{(1-f_\nu)f_{\nu_1}(1-f_{\nu_2})f_{\nu_3} - f_\nu(1-f_{\nu_1})f_{\nu_2}(1-f_{\nu_3})\} \\ &\times \delta(\varepsilon_\nu - \varepsilon_{\nu_1} + \varepsilon_{\nu_2} - \varepsilon_{\nu_3}). \end{aligned} \quad (1)$$

Two carriers are scattered out of states  $\nu_1$  and  $\nu_3$  into states  $\nu$  and  $\nu_2$  and vice versa. Scattering into a state  $\nu$  is proportional to the nonoccupation of that state  $(1-f_\nu)$  while scattering out of this state depends on the population  $f_\nu$ . Accordingly, the second and third line of Eq. (1) determine the availability of scattering partners. Since the scattering involves identical fermions, the scattering cross section is determined by screened Coulomb matrix elements for the direct and exchange interaction  $|W_{\nu\nu_2\nu_3\nu_1}|^2$  and  $W_{\nu\nu_2\nu_3\nu_1}W_{\nu\nu_2\nu_1\nu_3}^*$ , respectively. The total rate involves the sum over all possible scattering states  $\nu_1, \nu_2, \nu_3$ . The delta function in the last line of Eq. (1) ensures energy conservation.

## B. Wave functions and Coulomb matrix elements

The interaction matrix elements of the bare Coulomb potential  $v(\mathbf{r}-\mathbf{r}')$ ,

$$V_{\nu\nu_2\nu_3\nu_1} = \int d^3r d^3r' \Phi_\nu^*(\mathbf{r}) \Phi_{\nu_2}^*(\mathbf{r}') v(\mathbf{r}-\mathbf{r}') \Phi_{\nu_3}(\mathbf{r}') \Phi_{\nu_1}(\mathbf{r}), \quad (2)$$

contain the single-particle wave functions  $\Phi_\nu(\mathbf{r})$  of electrons and holes in the confinement potential of the combined QD-WL system. It is a complicated task on its own and beyond the scope of this paper to compute these single-particle states for a given confinement situation that depends on the QD geometry, the strain profile and possible composition variations within the QD.

As a simple model for the QD confinement, the wave functions within a three-dimensional box with infinitely high walls have been used in Ref. 6 to compute the Coulomb interaction matrix elements. Wojs *et al.*<sup>17</sup> have shown that for lens-shaped QD's on a WL with a QD height small in comparison to the QD diameter the in-plane component of the QD wave functions resembles in good approximation that of a two-dimensional harmonic oscillator. In the following we adopt this model for the (weak) in-plane confinement while for the (strong) confinement in the direction perpendicular to the WL a finite-height potential barrier will be used. To account for a finite energetic height of the QD confinement potential only localized states within a given energy range are considered.

In a WL devoid of QD's the states would be described by plane waves for the in-plane part, multiplied by the state corresponding to the finite-height barrier confinement for the

perpendicular direction. In the presence of the QDs this picture still holds as a good approximation far away from the dots. Close to the QD's, however, strong perturbations are expected, mainly due to the orthogonality requirement which brings in additional oscillations. Commonly<sup>6,18</sup> this situation is described by using the orthogonalized plane wave (OPW) scheme, summarized in Appendix A.

We consider an ensemble of identical QD's and assume that the states of different QD's are nonoverlapping. This is true for low QD densities where the mean QD spacing is much larger than the confinement length of the oscillator states. Another instance of interaction between QD's is provided by the Coulomb matrix elements. As shown below some scattering channels may, in principle, involve localized states belonging to different QD's. Nevertheless, these processes are limited to QD's less than a screening length apart. Considering a regime where the screening length is much smaller than the mean QD distance (sufficiently high carrier densities and/or sufficiently dilute QD's) no such interaction takes place. The theory can of course be extended beyond this regime of parameters, but this will not be done here.

The advantage of the discussed approximation scheme is that for all possible combinations of QD and WL states the Coulomb matrix elements can be determined to a large extent analytically. For a WL extending in the  $x$ - $y$  plane the separation of the wave function into in-plane and  $z$  components takes the form

$$\Phi_\nu(\mathbf{r}) = \varphi_l^b(\boldsymbol{\rho}) \xi_\sigma^b(z) u_b(\mathbf{r}), \quad (3)$$

where  $u_b(\mathbf{r})$  are Bloch functions. The quantum numbers for the in-plane and  $z$  components of the wave functions  $l$  and  $\sigma$ , respectively, as well as the band index  $b=e,h$  for electrons and holes are combined in  $\nu$ . With the help of the Fourier transform of the Coulomb potential, this factorization of the wave functions can be used to introduce in-plane Coulomb matrix elements with the two-dimensional momentum  $\mathbf{q}$ ,

$$\begin{aligned} V_{\sigma\sigma_2\sigma_3\sigma_1}^{b,b'}(\mathbf{q}) &= \frac{e^2}{2\varepsilon_0 q} \int dz dz' \\ &\times \xi_\sigma^b(z) \xi_{\sigma_2}^{b'}(z')^* e^{-q|z-z'|} \xi_{\sigma_3}^{b'}(z') \xi_{\sigma_1}^b(z) \end{aligned} \quad (4)$$

and Eq. (2) can be cast into the form

$$\begin{aligned} V_{\nu\nu_2\nu_3\nu_1} &= \frac{1}{A} \sum_{\mathbf{q}} V_{\sigma\sigma_2\sigma_3\sigma_1}^{b,b_2}(\mathbf{q}) \delta_{b,b_1} \delta_{b_2,b_3} \\ &\times \int d^2\rho \varphi_l^b(\boldsymbol{\rho}) \varphi_{l_1}^{b_1}(\boldsymbol{\rho}) e^{-i\mathbf{q}\cdot\boldsymbol{\rho}} \\ &\times \int d^2\rho' \varphi_{l_2}^{b_2}(\boldsymbol{\rho}') \varphi_{l_3}^{b_3}(\boldsymbol{\rho}') e^{i\mathbf{q}\cdot\boldsymbol{\rho}'}. \end{aligned} \quad (5)$$

It is seen that the in-plane space integrals over  $\boldsymbol{\rho}$  and  $\boldsymbol{\rho}'$  get separated, one involving the pair formed by the first and the last state, the other the pair formed by the second and the third state of the Coulomb matrix element. In the envelope function approximation, only pairs having the same band index ( $b=b_1$  and  $b_2=b_3$ ) contribute.

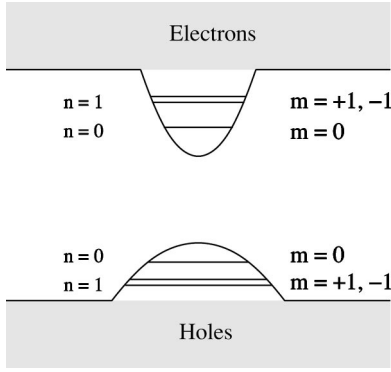


FIG. 1. Schematic drawing of energy levels in the quantum dot (QD) on wetting-layer (WL) system. The quasicontinuum of WL states (grey area) has larger interband transition energies than the discrete QD states labeled with the shell index  $n$  and the two-dimensional angular momentum  $m$ . The energetically degenerate states  $m = \pm 1$  are visualized by two separated lines.

While the above discussion is given for matrix elements of the bare Coulomb potential  $V_{\nu\nu_2\nu_3\nu_1}$ , the kinetic equation (1) contains screened Coulomb matrix elements  $W_{\nu\nu_2\nu_3\nu_1}$ . Within the approximations outlined in Appendix C screening due to WL carriers is included by multiplying Eq. (4) with a generalized quasi-two-dimensional inverse longitudinal dielectric function.

For the discrete QD states, the in-plane quantum numbers are  $l=(n,m)$  where  $n=0,1,2,\dots$  determines the energy ( $s,p,d,\dots$ , shell). In case of a two-dimensional harmonic confinement we have  $E_n^b=(n+1)E_{\text{QD}}^b$  for the QD energies where  $E_{\text{QD}}^b$  is the constant energy spacing between the shells. The second quantum number  $m=-n,-n+2,\dots,n-2,n$  characterizes the two-dimensional angular momentum. For QD's with confined  $s$  and  $p$  shell, these states are schematically shown in Fig. 1. For the quasicontinuum of WL states, the two-dimensional carrier momentum will be used as in-plane quantum numbers.

### C. Classification of scattering processes

The physical content of Eq. (1) will be more transparent if we decompose the summation over all quantum numbers  $\nu_1, \nu_2, \nu_3$  into subclasses. This grouping will depend upon whether a given state in the summation belongs to the extended WL or localized QD states. To indicate the particular choice,  $\nu$  will be replaced for QD states by the quantum number  $m$  ( $n$  is redundant as long as only  $s$  and  $p$  shells are considered) and the WL states are labeled by the in-plane momentum  $\mathbf{k}$ . The band indices of population functions  $f$  and energies  $\varepsilon$  will be explicitly given, all other quantum numbers are suppressed for notational simplicity.

For the three quantum numbers  $\nu_1, \nu_2, \nu_3$  in the kinetic equation (1) we find eight combinations between WL and QD states. In the following we discuss the changes of the QD population in the state  $\nu=m$ .

When WL states are used for the quantum numbers  $(\nu_1, \nu_2, \nu_3) = (\mathbf{k}_1, \mathbf{k}_2, \mathbf{k}_3)$ , the corresponding scattering rate of the kinetic equation describes carrier transitions between the

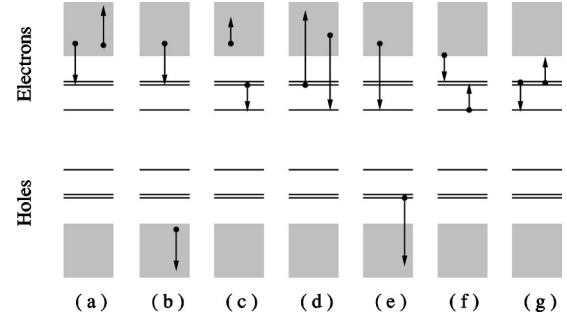


FIG. 2. Examples of scattering processes: (a) and (b) capture of electrons. (c) Relaxation process  $S^{(1)}$  for electrons. (d) Relaxation process  $S^{(2)}$  for electrons. (e) Mixed relaxation processes. (f) Capture and (g) relaxation process  $S^{(3)}$  assisted by QD carriers. The grey areas schematically show the energetic continua for delocalized states of electrons or holes while the three lines correspond to localized states.

WL and the QD state by means of other carriers scattered within the WL. Figures 2(a) and 2(b) show examples for the capture of electrons from the WL to the first excited QD state by means of scattering another electron or hole within the WL. The summation of all processes of this type which contribute to the right-hand side (RHS) of Eq. (1) is given by

$$S_{b,m}^{\text{cap}} = \frac{2\pi}{\hbar} \sum_{\mathbf{k}_1, \mathbf{k}_2, \mathbf{k}_3, b'} \delta(\varepsilon_m^b - \varepsilon_{\mathbf{k}_1}^b + \varepsilon_{\mathbf{k}_2}^{b'} - \varepsilon_{\mathbf{k}_3}^{b'}) \times W_{m\mathbf{k}_2\mathbf{k}_3\mathbf{k}_1} [2W_{m\mathbf{k}_2\mathbf{k}_3\mathbf{k}_1}^* - \delta_{b,b'} W_{m\mathbf{k}_2\mathbf{k}_1\mathbf{k}_3}^*] \times \{(1 - f_m^b) f_{\mathbf{k}_1}^b (1 - f_{\mathbf{k}_2}^{b'}) f_{\mathbf{k}_3}^{b'} - (f \rightarrow 1 - f)\}. \quad (6)$$

The first term in the third line of Eq. (6) accounts for the scattering out of states  $\mathbf{k}_1$  and  $\mathbf{k}_3$  into  $m$  and  $\mathbf{k}_2$  which increases the QD population. These processes are balanced with the reverse scattering events described by the second term in the third line of Eq. (6). Hence the net change of the QD population depends on the filling factors in both subsystems. In the following, we refer to this class of scattering events as *capture* processes.

Assuming that the WL population is independent of the carrier spin, the spin summation leads to a factor of 2 in the direct scattering term in the second line of Eq. (6). Note that the exchange term does not contribute for electron-hole scattering.

The summation over the scattering processes in Eq. (1) containing the matrix elements  $W_{m\mathbf{k}_1\mathbf{k}_2\mathbf{k}_3}$  and  $W_{m\mathbf{k}_1\mathbf{k}_2\mathbf{k}_3}$  can be decomposed into four separate groups of which three correspond to a redistribution of carriers between different QD levels (in the following called *QD relaxation*) by means of other WL carriers as shown in Figs. 2(c) and 2(d). The last group represents *mixed* scattering processes where, e.g., a hole is scattered out of a QD state into the WL while an electron is scattered from the WL into the QD, see Fig. 2(e).

The relaxation processes can be grouped in the following way:  $S_{\nu}^{\text{relax}} = S_{b,m}^{\text{1D}} + S_{b,m}^{\text{2D}} - S_{b,m}^{\text{12X}}$ . Here

$$S_{b,m}^{1D} = \frac{2\pi}{\hbar} \sum_{m_1, \mathbf{k}_2, \mathbf{k}_3, b'} 2|W_{m\mathbf{k}_2\mathbf{k}_3m_1}|^2 \delta(\varepsilon_m^b - \varepsilon_{m_1}^b + \varepsilon_{\mathbf{k}_2}^{b'} - \varepsilon_{\mathbf{k}_3}^{b'}) \times \{(1 - f_m^b) f_{m_1}^b (1 - f_{\mathbf{k}_2}^{b'}) f_{\mathbf{k}_3}^{b'} - (f \rightarrow 1 - f)\} \quad (7)$$

contains the direct Coulomb interaction for scattering of QD carriers between levels  $m$  and  $m_1$  by means of scattering either electrons or holes within the WL between states  $\mathbf{k}_2$  and  $\mathbf{k}_3$ .

A redistribution of carries within the QD also takes place when a carrier from the QD scatters to the WL while another carrier from a different WL state scatters back to a different QD level. Such a process is for electrons depicted in Fig. 2(d). The summation of all processes of this type due to direct Coulomb interaction is given by

$$S_{b,m}^{2D} = \frac{2\pi}{\hbar} \sum_{m_1, \mathbf{k}_2, \mathbf{k}_3} 2|W_{m\mathbf{k}_2m_1\mathbf{k}_3}|^2 \delta(\varepsilon_m^b - \varepsilon_{\mathbf{k}_3}^b + \varepsilon_{\mathbf{k}_2}^b - \varepsilon_{m_1}^b) \times \{(1 - f_m^b) f_{\mathbf{k}_3}^b (1 - f_{\mathbf{k}_2}^b) f_{m_1}^b - (f \rightarrow 1 - f)\}. \quad (8)$$

The Coulomb exchange contributions to the scattering processes described in Eqs. (7) and (8) can be combined to

$$S_{b,m}^{12X} = \frac{2\pi}{\hbar} \sum_{m_1, \mathbf{k}_2, \mathbf{k}_3} 2 \operatorname{Re}[W_{m\mathbf{k}_2\mathbf{k}_3m_1} W_{m\mathbf{k}_2m_1\mathbf{k}_3}^*] \times \{(1 - f_m^b) f_{m_1}^b (1 - f_{\mathbf{k}_2}^b) f_{\mathbf{k}_3}^b - (f \rightarrow 1 - f)\} \times \delta(\varepsilon_m^b - \varepsilon_{m_1}^b + \varepsilon_{\mathbf{k}_2}^b - \varepsilon_{\mathbf{k}_3}^b). \quad (9)$$

Finally we have so-called mixed scattering processes where, e.g., an electron is captured from the WL into a QD state by means of a hole which is scattered from a QD into the WL. Since the capture is typically faster for holes as will be discussed below, this process can be important to increase the electron capture with the help of already captured holes. The scattering rate is given by

$$S_{e,m}^{\text{mixed}} = \frac{2\pi}{\hbar} \sum_{m_1, \mathbf{k}_2, \nu_1, \mathbf{k}_3} 2|W_{m\mathbf{k}_2m_1\mathbf{k}_3}|^2 \delta(\varepsilon_m^e - \varepsilon_{\mathbf{k}_3}^e + \varepsilon_{\mathbf{k}_2}^h - \varepsilon_{m_1}^h) \times \{(1 - f_m^e) f_{\mathbf{k}_3}^e (1 - f_{\mathbf{k}_2}^h) f_{m_1}^h - (f \rightarrow 1 - f)\} \quad (10)$$

and similarly for the holes with ( $e \leftrightarrow h$ ).

The scattering processes discussed so far describe capture and relaxation *assisted by WL carriers*. Another class involves transitions of carriers *assisted by QD carriers*. Requirements for these processes are more restrictive since (i) the scattering partners provide only discrete energies which limits the range of possible transitions and (ii) populated initial and (sufficiently) unpopulated final states in the QD have to be available. As shown in the next section, efficient capture and relaxation processes can be provided even under quasiequilibrium conditions for intermediate carrier densities.

Capture processes assisted by QD carriers are described by

$$S_{b,m}^{\text{cap}'} = \frac{2\pi}{\hbar} \sum_{\mathbf{k}_1, m_2, m_3, b'} \delta(\varepsilon_m^b - \varepsilon_{\mathbf{k}_1}^b + \varepsilon_{m_2}^{b'} - \varepsilon_{m_3}^{b'}) \times W_{mm_2m_3\mathbf{k}_1} [2W_{mm_2m_3\mathbf{k}_1}^* - \delta_{b,b'} W_{mm_2\mathbf{k}_1m_3}^*] \times \{(1 - f_m^b) f_{\mathbf{k}_1}^b (1 - f_{m_2}^{b'}) f_{m_3}^{b'} - (f \rightarrow 1 - f)\}. \quad (11)$$

The first term in the third line accounts for the scattering out of states  $\mathbf{k}_1$  into the state  $m$  assisted by carriers scattered from states  $m_3$  into  $m_2$  which increases the QD population, see Fig. 2(f). Again balancing occurs with the reverse processes described by the second term of the third line. For processes involving solely electrons (or holes), energy conservation allows only capture from the WL to the excited QD states.

Relaxation processes assisted by QD carriers can be obtained from

$$S_{b,m}^{3DX} = \frac{2\pi}{\hbar} \sum_{m_1, \mathbf{k}_2, m_3, b'} \delta(\varepsilon_m^b - \varepsilon_{m_1}^b + \varepsilon_{\mathbf{k}_2}^{b'} - \varepsilon_{m_3}^{b'}) \times W_{m\mathbf{k}_2m_3m_1} [2W_{m\mathbf{k}_2m_3m_1}^* - \delta_{b,b'} W_{m\mathbf{k}_2m_1m_3}^*] \times \{(1 - f_m^b) f_{m_1}^b (1 - f_{\mathbf{k}_2}^{b'}) f_{m_3}^{b'} - (f \rightarrow 1 - f)\}. \quad (12)$$

Assuming that  $m$  and  $m_1$  label energetically lower and higher QD energies, respectively, carrier relaxation between these states takes place by means of another QD carrier  $m_3$  scattered into the WL state  $\mathbf{k}_2$ , see Fig. 2(g). In a situation where carrier capture is more efficient for excited QD states, this process is expected to contribute to the carrier relaxation within the QD.

There is yet another combination of QD and WL states contributing to QD-assisted processes

$$S_{b,m}^{4DX} = \frac{2\pi}{\hbar} \sum_{m_1, m_2, \mathbf{k}_3, b'} \delta(\varepsilon_m^b - \varepsilon_{m_1}^b + \varepsilon_{m_2}^{b'} - \varepsilon_{\mathbf{k}_3}^{b'}) \times W_{mm_2\mathbf{k}_3m_1} [2W_{mm_2\mathbf{k}_3m_1}^* - \delta_{b,b'} W_{mm_2m_1\mathbf{k}_3}^*] \times \{(1 - f_m^b) f_{m_1}^b (1 - f_{m_2}^{b'}) f_{\mathbf{k}_3}^{b'} - (f \rightarrow 1 - f)\}, \quad (13)$$

which describes, e.g., the carrier depletion of the excited QD states in connection with the relaxation processes of Eq. (12) or a transition into an excited QD state due to the assisting scattering partner for a capture processes of Eq. (11). It should be noted that the out-scattering events of Eqs. (11) and (13) are directly related to the in-scattering processes of Eq. (12) and vice versa. However, the rates contain summations over different states and different filling factors contributing to the scattering times introduced below.

In the notation of Eqs. (11)–(13) we assume that for the processes  $b=b'=e, h$  only  $\mathbf{k}=0$  WL states contribute (see below). Then nonvanishing Coulomb matrix elements are only obtained for different angular-momentum states of the two involved  $p$ -shell carriers. In this case both spin combinations of the assisting carriers are allowed which leads to the factor of two in the direct Coulomb terms. When other

WL states are involved and two  $p$ -shell carriers in the same angular-momentum states contribute, this factor and the exchange term need to be removed.

Scattering contributions involving the following Coulomb matrix elements are left out:  $W_{mm_1m_2m_3}$  corresponds to internal QD scattering and energy conserving processes do not change the population while terms containing  $W_{mm_1k_2k_3}$  cannot fulfill the energy conservation given by the delta function.

For the single-particle energies entering the scattering integrals, renormalization due to Coulomb interaction has been neglected. Energy shifts of several meV have been calculated for the (bare) Coulomb interaction of few carriers in a QD. The aim of this paper is, however, the description of the laser regime with a large carrier density in the WL. Efficient screening of WL carriers is expected to reduce the Coulomb shifts. One could argue that for nearby carriers (confined to the same QD) screening due to WL carriers is less efficient, but this has to be put in relation to the high WL carrier density we aim at. Simple Hartree-Fock energy renormalizations are known to strongly overestimate the energy shifts under high excitation conditions. Calculations beyond this level are an area of ongoing research in the field of quantum kinetics and beyond the scope of this paper.

#### D. Model system

For the numerical results presented in this paper we consider an InGaAs QD-WL system. Parabolic dispersion is assumed for conduction and valence bands with effective masses  $m_e=0.067m_0$  and  $m_h=0.15m_0$ , respectively, and the dielectric constant  $\epsilon=12.5$ . Unless otherwise noted, a 2.2 nm WL thickness and 2.1 nm additional QD height are used. The finite height of the confinement potential for electrons and holes is taken to be 350 and 170 meV, respectively, such that equal  $z$ -confinement wave functions  $\xi_{\sigma}^b(z)$  for electrons and holes can be adopted.

For a small WL thickness and QD height the energy spacing of the subbands and sublevels due to confinement in the  $z$  direction is large and only the lowest quantum number  $\sigma$  will be considered. Furthermore, we assume that the harmonic confinement potential leads to equal QD in-plane wave functions for electrons and holes. Different electron and hole masses then result in different level energies. We investigate QDs where the (double degenerate) ground state and the (fourfold degenerate) first excited state are confined. The energies of the ground state for electrons (holes) are 80 meV (30 meV) and for the first excited state 40 meV (15 meV) below the continuum of the WL. A density of QD's  $n_{\text{dot}}=10^{10} \text{ cm}^{-2}$  entering the OPW procedure discussed in Appendixes A and B will be used. Then, for the combined QD-WL system in thermodynamic equilibrium at 300 K, inversion of the lowest QD state as a precondition for optical gain is realized when the WL carrier density exceeds  $1.3 \times 10^{11} \text{ cm}^{-2}$ .

### III. RESULTS FOR COULOMB SCATTERING

#### A. Equilibrium scattering rates

As a general property, for any initial carrier distribution function the combined action of the discussed scattering pro-

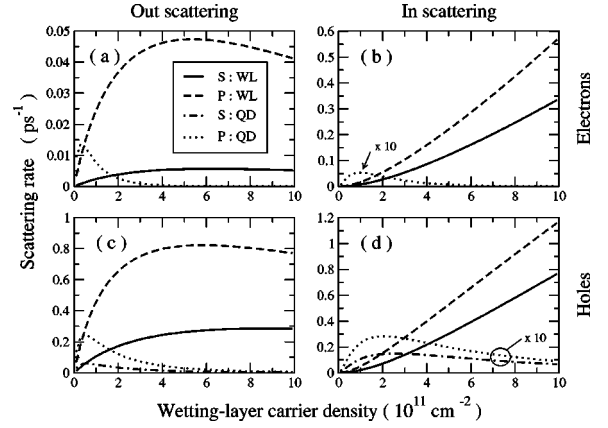


FIG. 3. Scattering rates for capture processes to QD ground states (solid and dashed-dotted lines: assisted by WL and QD carriers, respectively) and to first excited states (dashed and dotted lines: assisted by WL and QD carriers, respectively) for electrons (a), (b) and holes (c), (d) as a function of the carrier density in the WL at 300 K. In-scattering rates for processes assisted by QD carriers are scaled up for better visibility.

cesses will evolve the distribution functions of electrons and holes towards Fermi-Dirac functions where the QD and WL electrons and correspondingly the holes will have the same chemical potential  $\mu_e$  and  $\mu_h$ , respectively.

During such a time evolution towards equilibrium the relative importance of various scattering processes is expected to change via their dependence on the (nonequilibrium) carrier distribution functions for WL and QD states. To uniquely compare the influence of various processes, we assume that an equilibrium situation (at 300 K) has been reached and study the dependence of the scattering processes on the WL carrier density.

Equation (1) can be cast into the form

$$\frac{\partial}{\partial t} f_{\nu} = (1 - f_{\nu}) S_{\nu}^{\text{in}} - f_{\nu} S_{\nu}^{\text{out}}, \quad (14)$$

and based on the above classification we analyze in detail the in- and out-scattering rates  $S_{\nu}^{\text{in}}$  and  $S_{\nu}^{\text{out}}$  for capture, relaxation, and mixed processes.

In Fig. 3 the scattering rates for the electron and hole capture processes are shown. First we discuss results for the capture assisted by WL carriers. In scattering becomes more efficient for increasing WL carrier density. The same applies to out scattering up to intermediate WL carrier densities. In both cases the scattering rate increases due to the larger population of available scattering partners. When the population of the energetically lower WL states approaches unity, Pauli blocking starts to reduce the out scattering, i.e., the reverse of the processes schematically depicted in Figs. 2(a) and 2(b), due to the reduction of available final states. The population factors might still allow WL carriers at higher energies to assist the QD-WL scattering. Their contribution is, however, strongly reduced due to the Gaussian decay of the Coulomb interaction matrix elements with the WL carrier momenta.

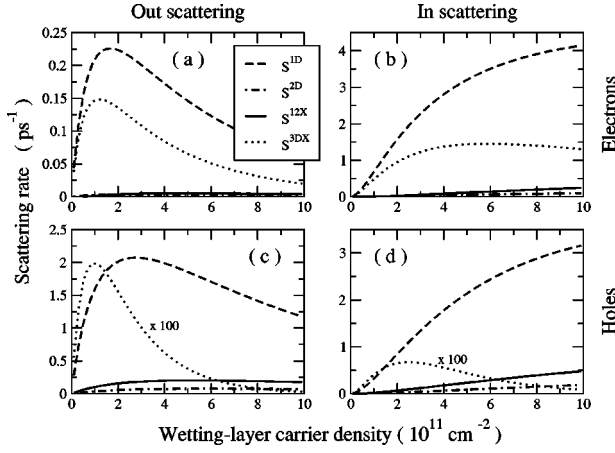


FIG. 4. Scattering rates for QD carrier relaxation processes according to Eqs. (7)–(9) and (12). (a) and (c) represent scattering out of the QD ground state into the QD excited states while (b) and (d) show results for the reverse processes.

Processes assisted by QD carriers are only important in an intermediate density range and are typically weaker than the processes assisted by WL carriers. For low carrier densities the initial states of the assisting scattering partners are not populated and for higher carrier densities Pauli blocking prevents scattering into possible final QD states. (Note that we assume a quasiequilibrium situation for the coupled QD-WL system.) For the used level spacing, energy conservation does not allow electron capture to the  $s$  shell by means of QD electrons or holes while capture of holes to the  $s$  shell is possible by means of QD electrons.

Generally, the processes related to the QD ground states are slower than those for the first excited QD states since the larger energy difference requires WL carriers with larger momenta which again leads to smaller Coulomb interaction matrix elements. For the same reason, the corresponding scattering rates for holes are larger than for electrons. In earlier references, exchange contributions to the scattering rates are often omitted. For processes assisted by WL carriers curves without exchange interaction exhibit a similar shape but results are overestimated by about 20 (10%) for the  $p$  ( $s$ ) shell, respectively. For processes assisted by QD carriers direct and (possible) exchange Coulomb matrix elements are equal. Hence, contributing exchange terms reduce the scattering rates for these channels by 50%.

The scattering rates for various relaxation processes are shown in Fig. 4. In and out scattering refer to the QD ground states. When the relaxation processes involve only two (degenerate) confined levels, the corresponding out-scattering rate for the ground state equals the in-scattering rate due to relaxation for the excited state and vice versa.

Processes assisted by WL and QD carriers will be discussed separately. Regarding the first class, the qualitative behavior of the WL carrier density dependence for in and out scattering is similar to the capture processes for the reasons discussed above. In all cases  $S^{1D}$  provides the dominant contribution while  $S^{2D}$  and  $S^{12X}$  are much smaller. Since  $S^{2D}$  and  $S^{12X}$  contribute with opposite sign, they partly compensate each other. The  $S^{1D}$  relaxation rates dominate mainly because

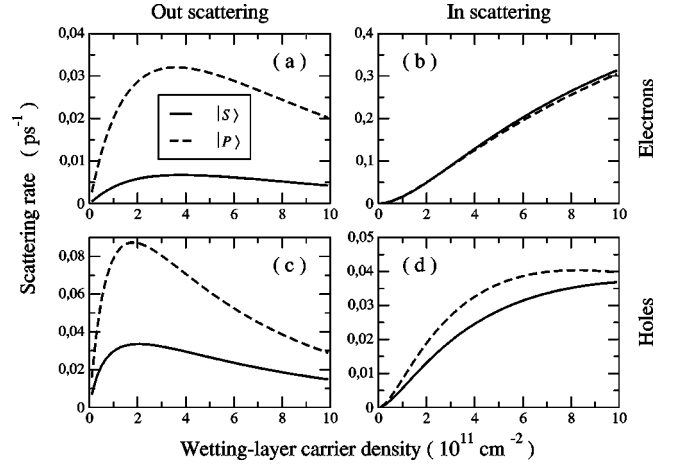


FIG. 5. Rates for mixed scattering processes. (a) and (b) show electron in and outscattering while (c) and (d) are hole in and outscattering, respectively.

the Coulomb interaction matrix elements make it more favorable to scatter between two QD carriers assisted by a transition between two WL carriers, in comparison to two coupled transitions between QD and WL carriers. Furthermore,  $S^{1D}$  also contains electron-hole scattering which does not contribute to  $S^{2D}$  and  $S^{12X}$ .

For the comparison of scattering rates of electrons and holes, two counteracting contributions need to be considered. The energy spacing between QD states is smaller for holes which increases their scattering rates. The smaller population of holes due to their larger effective mass, on the other hand, decreases their in-scattering rate and increases their out-scattering rate. As a result, the in-scattering rates of electrons and holes are comparable while the out-scattering rates are larger for holes.

The relaxation processes assisted by QD carriers require a rather detailed discussion. The rates depend more strongly on the QD energy spacing in comparison to the energetic distance of the excited QD states from the WL continuum. For the used example, relaxation of electrons assisted by QD electrons (ditto for holes) according to Eq. (12) involves only the  $\mathbf{k}=0$  WL state. This requires  $p$ -shell carriers in opposite angular-momentum states for  $m_1$  and  $m_3$  to obtain nonvanishing Coulomb matrix elements. On the other hand, electron relaxation assisted by holes allows  $\mathbf{k} \neq 0$  and also the same angular-momentum states for  $m_1$  and  $m_3$  contribute. The corresponding Coulomb matrix elements can be up to an order of magnitude larger (in comparison to the  $\mathbf{k}=0$  matrix elements) depending on the involved WL momentum. Hence, the large rate  $S^{3DX}$  for electrons is due to efficient  $e$ - $h$  scattering while energy conservation does not allow  $h$ - $e$  contributions to the hole relaxation and the  $h$ - $h$  process involving  $\mathbf{k}=0$  is weak. While this situation clearly changes with different spacing of the excited QD states from the WL continuum, the obtained relaxation rates for electrons and holes can be considered as limiting cases (other choices for the QD energy levels are typically in between these extremes).

In Fig. 5 the mixed scattering rates are shown in the same notation used in Fig. 4. Finding the same WL carrier-density dependence as above, we notice however that in-scattering

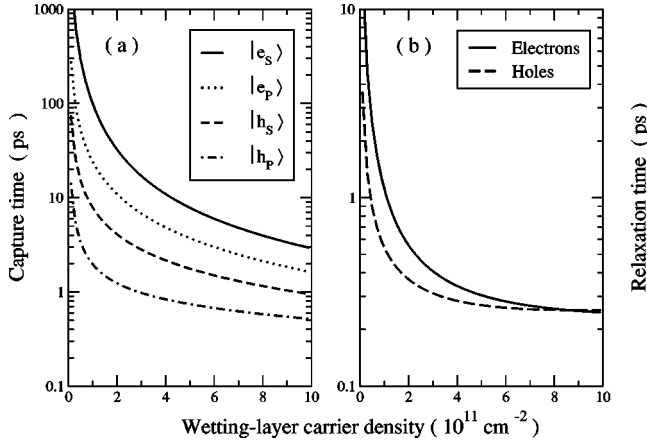


FIG. 6. Scattering times for processes assisted by WL carriers. (a) Capture times for WL carriers to the QD ground states  $|e_s\rangle$  and first excited states  $|e_p\rangle$  for electrons and correspondingly for holes. (b) Relaxation times for carrier scattering from first excited states to ground states. The temperature is 300 K. Different axis scaling for capture and relaxation times should be noted.

processes are faster for electrons than for holes. Scattering an electron from the bottom of the WL into the QD ground state, as schematically shown in Fig. 2(e), puts a QD hole far up in the valence band WL (where the final state population is small) due to the larger QD confinement energy for electrons. The probability for the reverse process (hole in scattering) is strongly reduced due to the small initial-state population for holes and large final-state population for electrons.

### B. Equilibrium capture and relaxation times

In- or out-scattering rates alone determine the population changes of the considered QD states when these states are completely empty or completely populated, respectively, as can be seen from Eq. (14). On the other hand, when all QD and WL states are in thermodynamic equilibrium with Fermi-Dirac distribution functions  $F_\nu$ , characteristic scattering times  $\tau_\nu$  can be introduced in response to small perturbations  $\delta f_\nu$ . Solving the kinetic equation (14) for a carrier distribution function  $f_\nu = F_\nu + \delta f_\nu$  we assume that the influence of  $\delta f_\nu$  on the scattering rates  $S_\nu^{\text{in}}$  and  $S_\nu^{\text{out}}$  can be neglected:

$$\frac{\partial}{\partial t} f_\nu = -\frac{f_\nu - F_\nu}{\tau_\nu}, \quad \frac{1}{\tau_\nu} = (S_\nu^{\text{in}} + S_\nu^{\text{out}}) F_\nu. \quad (15)$$

(For example, when  $f_\nu$  and  $F_\nu$  correspond to the same total carrier density,  $\delta f_\nu$  is a symmetric perturbation which tends to averages out in the scattering integrals.) Then the inverse of the scattering time  $\tau_\nu$  is given by the sum of in- and out-scattering rates calculated with the RHS of Eq. (1) using Fermi-Dirac functions, i.e., the scattering rates discussed in the previous subsection. The scattering time  $\tau_\nu$  determines the evolution back to equilibrium.

In Fig. 6(a) capture times calculated from the in- and out-scattering rates of Eq. (6) are shown, Fig. 6(b) contains the relaxation times according to Eqs. (7)–(9). The decreasing scattering times for increasing WL carrier density and the

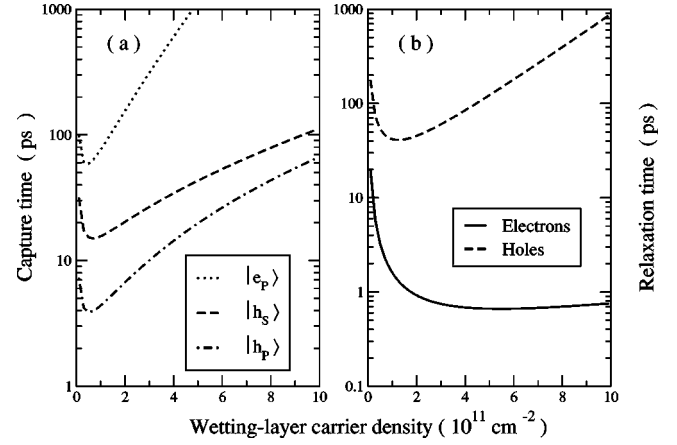


FIG. 7. Same as Fig. 6 but for processes assisted by QD carriers.

relative magnitude of the displayed capture and relaxation processes can be directly traced back to the above given detailed discussion of the scattering rates. The nearly constant hole relaxation time for WL carrier densities between  $4 \times 10^{11}$  and  $10^{12} \text{ cm}^{-2}$  is a result of the interplay of filling factors leading to a decreasing out-scattering rate and increasing in-scattering rate shown in Fig. 4.

As a function of carrier density the capture processes assisted by QD carriers, Fig. 7(a), initially dominate in comparison to the WL assisted ones in a range where both types of processes are slow. For intermediate to high carrier densities processes assisted by WL carriers provide the main capture channels. The results in Fig. 7(b) show only slightly smaller efficiency for the electron relaxation assisted by QD carriers in comparison to WL assisted processes. However, the values in Fig. 7(b) depend on the QD-QD vs QD-WL energy spacing. For other parameters, relaxation of holes can be as fast as for electrons but times are typically larger than for relaxation assisted by WL carriers.

The computed scattering times suggest the following dynamical scenario for the chosen material system. WL carriers

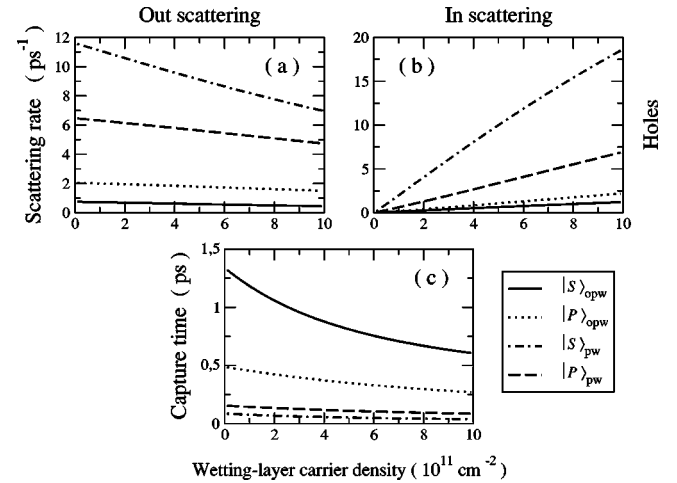


FIG. 8. (a), (b) Scattering rates for hole capture from the WL to the QD ground states (solid line: OPW, dashed-dotted line: PW) and to first excited states (dotted line: OPW, dashed line: PW) and corresponding capture times (c) at 300 K.

are dominantly captured to the excited states. Filling of the QD ground states occurs on almost the same time scale due to fast relaxation of carriers within the QD. Electronic capture processes are an order of magnitude slower than the corresponding processes for holes. Direct capture to the hole QD ground states also weakly contributes while direct capture to the electron QD ground state can be neglected for the considered large energy difference between the electron QD ground state and the WL.

#### IV. THEORY AND RESULTS FOR CARRIER-PHONON INTERACTION

In this section we consider the interaction of carriers with LO phonons. In the Markov approximation the kinetic equation determining the changes of the carrier population  $f_\nu$  is given by

$$\begin{aligned} \frac{\partial}{\partial t} f_\nu = & \frac{2\pi}{\hbar} \frac{M_{\text{LO}}^2}{e^2/\epsilon_0} \sum_{\nu'} W_{\nu'\nu\nu'} \\ & \times \{ (1-f_\nu) f_{\nu'} [(1+n_{\text{LO}}) \delta(\epsilon_\nu - \epsilon_{\nu'} + \hbar\omega_{\text{LO}}) \\ & + n_{\text{LO}} \delta(\epsilon_\nu - \epsilon_{\nu'} - \hbar\omega_{\text{LO}})] \\ & - f_\nu (1-f_{\nu'}) [n_{\text{LO}} \delta(\epsilon_\nu - \epsilon_{\nu'} + \hbar\omega_{\text{LO}}) \\ & + (1+n_{\text{LO}}) \delta(\epsilon_\nu - \epsilon_{\nu'} - \hbar\omega_{\text{LO}})] \}, \end{aligned} \quad (16)$$

where  $\omega_{\text{LO}}$  is the LO-phonon frequency. For the phonon population  $n_{\text{LO}}$  a Bose-Einstein function at the lattice temperature will be used to describe the crystal lattice in thermodynamic equilibrium. The Fröhlich coupling has been formulated in a general eigenfunction basis with the Coulomb matrix elements, Eq. (2). Hence, the calculation of the polar-coupling interaction matrix elements for WL and QD states can be done along the lines of Sec. II and Appendix B. The coupling constant  $M_{\text{LO}} = (e^2/\epsilon_0)(1/\epsilon_\infty - 1/\epsilon)(\hbar\omega_{\text{LO}}/2)$  contains the static and high-frequency relative dielectric constants  $\epsilon$  and  $\epsilon_\infty$ , respectively.  $M_{\text{LO}}$  can be expressed in terms of the dimensionless coupling constant  $\alpha = (e^2/4\pi\epsilon_0\hbar)\sqrt{m/2\hbar\omega_{\text{LO}}}(1/\epsilon_\infty - 1/\epsilon)$  with the reduced electron-hole-mass  $m$ .

Various terms on the RHS of Eq. (16) describe the scattering of carriers from states  $\nu$  into  $\nu'$  under the emission and absorption of an LO phonon as well as the reverse processes. Under the assumption of strict energy conservation, carrier relaxation between the QD states is only possible when the LO-phonon energy matches the level spacing. Furthermore, contributions to carrier capture are obtained only for an energy difference between the QD states and the WL larger than  $\hbar\omega_{\text{LO}}$ .

For our InGaAs system with  $\hbar\omega_{\text{LO}} = 36$  meV and  $\alpha = 0.06$  only hole capture is possible. According to Fig. 8, capture to both  $p$  and  $s$  shells is possible with an in-scattering rate comparable to the hole capture due to Coulomb scattering in Fig. 3 which shows also a similar WL carrier density dependence. Note that the capture *time* is defined according to Eq. (15) as the response time of the system to small perturbations from equilibrium and, hence, contains both in- and out-scattering rates. Since the out-scattering rate only weakly

depends on the WL carrier-density, the same holds for the capture time. In addition to the results obtained with OPW wave functions for the WL states (solid and dotted lines) also the plane-wave (PW) results are given (dashed and dashed-dotted lines). In this case the rates are strongly overestimated which emphasises again the importance of the OPW scheme discussed in Appendixes A and B.

In Refs. 11 and 12 also two-phonon processes have been studied based on Fermi's golden rule. For weak polar coupling, their efficiency is clearly reduced in comparison to one-phonon processes. Furthermore, in a perturbational treatment state filling effects of the intermediate states is neglected, which further reduces the scattering efficiency.

#### V. CONCLUSIONS

We have discussed in- and out-scattering rates as well as scattering times for capture and relaxation processes in the QD-WL system. In general, in- and out-scattering rates enter in a kinetic equation (14) from which the population dynamics for a given initial situation can be determined. The in-scattering rates solely describe the population changes as long as the final-state population can be neglected. This situation is closely connected to calculations based on Fermi's golden rule where fully populated initial states and empty final states are assumed. In an intermediate situation with existing final-state population, capture and relaxation processes will be less efficient due to Pauli blocking as well as out-scattering contributions. For completely filled states, the discussed out scattering rates solely determine the population losses.

On the other hand, the given scattering times characterize relaxation and capture processes under the assumption that *all* states are populated according to Fermi-Dirac statistics. The carriers in a laser operating under cw conditions are typically near a quasiequilibrium distribution. If, for example, the stimulated recombination depletes the lower QD states then the QD relaxation time determines the refilling of this state with carriers from the excited QD states and the capture times determine the refilling from the WL.

For the processes due to Coulomb interaction, relaxation within the QD is typically on a faster time scale than the carrier capture from the WL into the QD. Processes involving holes are typically faster than the corresponding processes involving electrons and capture to the excited states is faster than capture to the ground states. Hence in a dynamical scenario, first the holes are captured to the excited QD states and immediately scattered via relaxation to the QD ground states. Capture of electrons is somewhat slower, the subsequent relaxation for electrons is only slightly slower than for holes. When capture processes due to emission of LO phonons are possible, their efficiency is comparable to Coulomb scattering at elevated WL carrier densities.

Depending on the density of QD's the capture and relaxation processes in turn will change the WL carrier distribution. Together with the different time scales of the discussed processes involving QD carriers, a nontrivial interplay in dynamical situations is expected.

One of the goals of the paper is to study the influence of terms often neglected previously. In addition to the above

summarized interplay of in and out scattering and scattering times it is shown that the Coulomb vertex contributions typically cannot be neglected in comparison to the direct Coulomb interaction. Scattering processes assisted by QD carriers contribute especially at lower carrier densities and can add to the relaxation at higher densities. The use of WL wave functions properly orthogonalized to the QD states is found to be important for the evaluation of scattering rates. The relative contribution of OPW corrections depends on how the density of QD's enters. In the discussed Coulomb matrix elements for carrier capture and for relaxation (except in  $S^{1D}$ ) the orthogonalization even contributes if one would have a single QD in an infinite system, i.e., for zero QD density. Results for these processes based on plane wave WL states can strongly deviate from OPW calculations. On the other hand, screening due to WL carriers is somewhat less influenced by OPW corrections since the derived generalized Lindhard formula for OPW states contains the PW result plus corrections starting in first power of the QD density. Essentially, screening is a "global" effect less influenced by a small number of QDs whereas processes in the QD depend on the "local" features of the wave function. Here the orthogonalization is more important, because it changes the wave function exactly in the region of the QD where the transitions take place.

#### ACKNOWLEDGMENTS

We thank H.C. Schneider for valuable discussions. This work was supported by the Deutsche Forschungsgemeinschaft and with a grant for CPU time at the Forschungszentrum Jülich.

#### APPENDIX A: ORTHOGONALIZATION PROCEDURE

Our starting point for the construction of wave functions are WL states in the absence of QD's, which are considered as plane-waves  $\varphi_{\mathbf{k}}^0(\mathbf{r}) = (1/\sqrt{A})e^{i\mathbf{k}\cdot\mathbf{r}}$  with two-dimensional carrier momentum  $\mathbf{k}$ . To describe the combined system we use plane waves orthogonalized to the QD states (OPW)<sup>6,18</sup>

$$|\varphi_{\mathbf{k}}\rangle = \frac{1}{N_{\mathbf{k}}} \left( |\varphi_{\mathbf{k}}^0\rangle - \sum_{\alpha} |\varphi_{\alpha}\rangle \langle \varphi_{\alpha} | \varphi_{\mathbf{k}}^0 \rangle \right), \quad (\text{A1})$$

where  $N_{\mathbf{k}}$  is the normalization constant. The sum includes all localized states. In the following we assume an ensemble of identical, independent QD's with nonoverlapping wave functions. Then  $\alpha = (m, \mathbf{R})$  contains various QD states  $m$  at different QD positions  $\mathbf{R}$ . The QD states are thus mutually orthogonal  $\langle \varphi_{\alpha} | \varphi_{\alpha'} \rangle = \delta_{\alpha, \alpha'}$ .

By construction the OPW states for the WL are orthogonal to the QD states,  $\langle \varphi_{\alpha} | \varphi_{\mathbf{k}} \rangle = 0$ . To study the orthogonality of OPW states, we use

$$\langle \varphi_{\mathbf{k}} | \varphi_{\mathbf{k}'} \rangle = \frac{1}{N_{\mathbf{k}} N_{\mathbf{k}'}} \left( \langle \varphi_{\mathbf{k}}^0 | \varphi_{\mathbf{k}'}^0 \rangle - \sum_{\alpha} \langle \varphi_{\mathbf{k}}^0 | \varphi_{\alpha} \rangle \langle \varphi_{\alpha} | \varphi_{\mathbf{k}'}^0 \rangle \right). \quad (\text{A2})$$

As the plane wave overlap integrals with the QD states at different positions differ only by a phase

factor  $\langle \varphi_{\alpha} | \varphi_{\mathbf{k}}^0 \rangle = \int d^2 \varrho \varphi_m(\mathbf{r} - \mathbf{R}) \varphi_{\mathbf{k}}^0(\mathbf{r}) = \int d^2 \varrho \varphi_m(\mathbf{r}) \varphi_{\mathbf{k}}^0(\mathbf{r} + \mathbf{R}) \equiv \langle \varphi_m | \varphi_{\mathbf{k}}^0 \rangle e^{i\mathbf{k}\cdot\mathbf{R}}$ , we have

$$\langle \varphi_{\mathbf{k}} | \varphi_{\mathbf{k}'} \rangle = \frac{1}{N_{\mathbf{k}} N_{\mathbf{k}'}} \left( \delta_{\mathbf{k}, \mathbf{k}'} - \sum_{m, \mathbf{R}} \langle \varphi_{\mathbf{k}}^0 | \varphi_m \rangle \langle \varphi_m | \varphi_{\mathbf{k}'}^0 \rangle e^{i(\mathbf{k}' - \mathbf{k})\cdot\mathbf{R}} \right). \quad (\text{A3})$$

The sum over  $\mathbf{R}$  now involves only the phase factors. For randomly distributed QDs these phase factors will average to zero except for  $\mathbf{k} = \mathbf{k}'$ . More precisely, in the large area limit ( $A \rightarrow \infty$  with the number of QD's  $N \rightarrow \infty$  such that the QD density  $n_{\text{dot}} = N/A$  remains constant) one has

$$\frac{1}{N} \sum_{\mathbf{R}} e^{i(\mathbf{k}' - \mathbf{k})\cdot\mathbf{R}} = \delta_{\mathbf{k}, \mathbf{k}'}. \quad (\text{A4})$$

Hence, "on average," different OPW states are also orthogonal with the normalization

$$N_{\mathbf{k}} = \sqrt{1 - N \sum_m |\langle \varphi_{\mathbf{k}}^0 | \varphi_m \rangle|^2}. \quad (\text{A5})$$

Using the normalization area  $A$  of the plane waves, the prefactor of the sum over the QD states is accordingly given by the QD density  $n_{\text{dot}}$ .

#### APPENDIX B: COULOMB MATRIX ELEMENTS

When the first and last or the second and third arguments of the Coulomb matrix elements belong to OPW states, the corresponding in-plane integrals in Eq. (5) can be explicitly calculated using Eq. (A1):

$$\begin{aligned} \langle \varphi_{\mathbf{k}} | e^{i\mathbf{q}\cdot\mathbf{r}} | \varphi_{\mathbf{k}'} \rangle &= \frac{1}{N_{\mathbf{k}} N_{\mathbf{k}'}} \left( \langle \varphi_{\mathbf{k}}^0 | e^{i\mathbf{q}\cdot\mathbf{r}} | \varphi_{\mathbf{k}'}^0 \rangle \right. \\ &+ \sum_{\alpha, \alpha'} \langle \varphi_{\mathbf{k}}^0 | \varphi_{\alpha} \rangle \langle \varphi_{\alpha} | e^{i\mathbf{q}\cdot\mathbf{r}} | \varphi_{\alpha'} \rangle \langle \varphi_{\alpha'} | \varphi_{\mathbf{k}'}^0 \rangle \\ &- \sum_{\alpha} \langle \varphi_{\mathbf{k}}^0 | e^{i\mathbf{q}\cdot\mathbf{r}} | \varphi_{\alpha} \rangle \langle \varphi_{\alpha} | \varphi_{\mathbf{k}'}^0 \rangle \\ &\left. - \sum_{\alpha} \langle \varphi_{\mathbf{k}}^0 | \varphi_{\alpha} \rangle \langle \varphi_{\alpha} | e^{i\mathbf{q}\cdot\mathbf{r}} | \varphi_{\mathbf{k}'}^0 \rangle \right). \quad (\text{B1}) \end{aligned}$$

Again, in the large area limit the random QD distribution restores the translation invariance (momentum conservation) of the problem, and one obtains

$$\begin{aligned} \langle \varphi_{\mathbf{k}} | e^{i\mathbf{q}\cdot\mathbf{r}} | \varphi_{\mathbf{k}'} \rangle &= \delta_{\mathbf{k} - \mathbf{q} - \mathbf{k}'} \frac{1}{N_{\mathbf{k}} N_{\mathbf{k}'}} \\ &\times \left( 1 - N \sum_m |\langle \varphi_{\mathbf{k}}^0 | \varphi_m \rangle|^2 - N \sum_m |\langle \varphi_m | \varphi_{\mathbf{k}'}^0 \rangle|^2 \right. \\ &\left. + N \sum_{m, m'} \langle \varphi_{\mathbf{k}}^0 | \varphi_m \rangle \langle \varphi_m | e^{i\mathbf{q}\cdot\mathbf{r}} | \varphi_{m'} \rangle \langle \varphi_{m'} | \varphi_{\mathbf{k}'}^0 \rangle \right), \quad (\text{B2}) \end{aligned}$$

where the remaining overlap integrals of localized QD wave functions and plane waves can be calculated analytically for harmonic oscillator states.

In the case when the pairing of the states in the Coulomb matrix elements involves one OPW state and one QD state the in-plane integrals in Eq. (5) lead to

$$\begin{aligned} \langle \varphi_\alpha | e^{i\mathbf{q}\cdot\boldsymbol{\rho}} | \varphi_{\mathbf{k}} \rangle &= \frac{1}{N_{\mathbf{k}}} \left( \langle \varphi_\alpha | e^{i\mathbf{q}\cdot\boldsymbol{\rho}} | \varphi_{\mathbf{k}}^0 \rangle \right. \\ &\quad \left. - \sum_{\alpha'} \langle \varphi_\alpha | e^{i\mathbf{q}\cdot\boldsymbol{\rho}} | \varphi_{\alpha'} \rangle \langle \varphi_{\alpha'} | \varphi_{\mathbf{k}}^0 \rangle \right). \end{aligned} \quad (\text{B3})$$

With the above given arguments we find for a QD at position  $\mathbf{R}$  that  $\langle \varphi_\alpha | e^{i\mathbf{q}\cdot\boldsymbol{\rho}} | \varphi_{\mathbf{k}}^0 \rangle = \int d^2\boldsymbol{\rho} \varphi_m(\boldsymbol{\rho} - \mathbf{R}) e^{i\mathbf{q}\cdot\boldsymbol{\rho}} \varphi_{\mathbf{k}}^0(\boldsymbol{\rho}) = \langle \varphi_m | \varphi_{\mathbf{k}+\mathbf{q}}^0 \rangle e^{i(\mathbf{k}+\mathbf{q})\cdot\mathbf{R}}$ . Since we neglect the wave function overlap of different QD's, this results in

$$\begin{aligned} \langle \varphi_\alpha | e^{i\mathbf{q}\cdot\boldsymbol{\rho}} | \varphi_{\mathbf{k}} \rangle &= \frac{1}{N_{\mathbf{k}}} \left( \langle \varphi_m | \varphi_{\mathbf{k}+\mathbf{q}}^0 \rangle \right. \\ &\quad \left. - \sum_{m'} \langle \varphi_m | e^{i\mathbf{q}\cdot\boldsymbol{\rho}} | \varphi_{m'} \rangle \langle \varphi_{m'} | \varphi_{\mathbf{k}}^0 \rangle \right) e^{i(\mathbf{k}+\mathbf{q})\cdot\mathbf{R}}. \end{aligned} \quad (\text{B4})$$

Hence for QD's at positions  $\mathbf{R}$ , phase factors  $e^{i(\mathbf{k}+\mathbf{q})\cdot\mathbf{R}}$  enter the Coulomb matrix elements of the discussed structure which contribute in Eqs. (6) and (8)–(10). When the capture of carriers in a particular QD is calculated from Eq. (6) these phase factors cancel exactly, i.e., the processes are independent of the QD position. The same applies when carriers are scattered within the same QD according to Eqs. (8)–(10). It should be noted that the first Coulomb matrix element in Eq. (9) requires that the two QD quantum numbers  $m$  and  $m_1$  belong to the same QD position as long as the wave function overlap between different QD's vanishes. For the same reason, Eq. (7) describes only carrier scattering within the same QD. However, Coulomb interaction can couple carriers in different QD's (even for vanishing overlap of their wave functions) according to processes described in Eqs. (8) and (10) and depicted in Figs. 2(d) and 2(e) where a carrier from one QD is scattered into the WL while another carrier from the WL is scattered into a different QD. It can be seen by direct inspection of Eq. (2) that these matrix elements are controlled by the strength of the Coulomb interaction at the distance between the two QD's involved. Hence the screening length of the Coulomb interaction in comparison to the QD separation limits these processes. In this paper we assume sufficiently large screening of the Coulomb interaction due to WL carriers in order to neglect these processes. (For a typical WL carrier density of  $10^{11} \text{ cm}^{-2}$  at 300 K the Debye screening length is 0.76 in units of the  $3d$  exciton Bohr radius.) Therefore, Eqs. (6)–(13) describe scattering processes involving each QD separately and taking place identically in all QD's.

### APPENDIX C: SCREENING OF THE COULOMB INTERACTION

While the discussion of interaction matrix elements in Sec. II B refers to the bare Coulomb potential, the effect of screening will be included in the following. The screened

Coulomb interaction  $w(\mathbf{r}_1, \mathbf{r}_2)$  obeys the integral equation

$$w(\mathbf{r}_1, \mathbf{r}_2) = v(\mathbf{r}_1 - \mathbf{r}_2) + \int d^3r_3 d^3r_4 v(\mathbf{r}_1 - \mathbf{r}_3) P(\mathbf{r}_3, \mathbf{r}_4) w(\mathbf{r}_4, \mathbf{r}_2) \quad (\text{C1})$$

with the bare Coulomb interaction  $v(\mathbf{r} - \mathbf{r}')$  and the longitudinal polarization  $P(\mathbf{r}, \mathbf{r}')$ .<sup>19</sup> In the equilibrium situation discussed in this paper,  $w$  and  $P$  additionally depend on the frequency  $\omega$  in connection with dynamical screening effects. In a nonstationary situation treated in Markov approximation, they furthermore depend on the macroscopic time  $t$ . For notational simplicity, these arguments are omitted.

The random-phase approximation<sup>19</sup> for the longitudinal polarization leads to the eigenfunction expansion  $P(\mathbf{r}, \mathbf{r}') = \sum_{\nu\nu'} \Phi_\nu(\mathbf{r}) \Phi_{\nu'}(\mathbf{r}') P_{\nu\nu'} \Phi_\nu^*(\mathbf{r}') \Phi_{\nu'}^*(\mathbf{r})$ . In the above discussed limit of large WL carrier densities and/or small density of QDs on the WL we consider only screening of the Coulomb interaction due to WL carriers, i.e.,  $\nu$  and  $\nu'$  are WL states. With the OPW description of the previous appendices, the WL states are ‘‘on average’’ spatially homogeneous and the longitudinal polarization possesses in-plane translational invariance. This can be directly seen from

$$\begin{aligned} &\int d^2\boldsymbol{\rho} \int d^2\boldsymbol{\rho}' e^{-i\mathbf{q}\cdot\boldsymbol{\rho}} P(\mathbf{r}, \mathbf{r}') e^{i\mathbf{q}'\cdot\boldsymbol{\rho}'} \\ &= \sum_{\mathbf{k}, \mathbf{k}'} \langle \varphi_{\mathbf{k}'} | e^{-i\mathbf{q}\cdot\boldsymbol{\rho}} | \varphi_{\mathbf{k}} \rangle \langle \varphi_{\mathbf{k}} | e^{i\mathbf{q}'\cdot\boldsymbol{\rho}'} | \varphi_{\mathbf{k}'} \rangle P_{\mathbf{k}, \mathbf{k}'}(z, z') \\ &= \delta_{\mathbf{q}, \mathbf{q}'} \sum_{\mathbf{k}} P_{\mathbf{k}, \mathbf{k}-\mathbf{q}}(z, z') |F_{\mathbf{k}, \mathbf{k}-\mathbf{q}}|^2, \end{aligned} \quad (\text{C2})$$

where in the eigenfunction expansion only the in-plane components of the wave functions has been used. For the evaluation of the overlap integrals involving OPW states we have introduced the short notation

$$\langle \varphi_{\mathbf{k}} | e^{-i\mathbf{q}\cdot\boldsymbol{\rho}} | \varphi_{\mathbf{k}'} \rangle = \delta_{\mathbf{k}-\mathbf{q}, \mathbf{k}'} F_{\mathbf{k}, \mathbf{k}'}, \quad (\text{C3})$$

where  $F_{\mathbf{k}, \mathbf{k}'}$  can be obtained from a comparison with Eq. (B2) and describes the OPW corrections of the plane-wave result.

Already at this point one can conclude [e.g., from an iterative solution of Eq. (C1) with the structure  $w = v + vPv + vPvPv + \dots$ ] that since  $P(\mathbf{r}, \mathbf{r}') = P(\boldsymbol{\rho} - \boldsymbol{\rho}', z, z')$ , the screened Coulomb interaction depends also only on the difference of the in-plane space arguments. This behavior is to be expected on intuitive grounds since we consider a uniform distribution of QD's that translates into in-plane homogeneity of the screened Coulomb interaction. The property essentially simplifies the following calculation of screened Coulomb matrix elements along the lines demonstrated for the bare Coulomb interaction in Eqs. (2)–(5).

Our starting point is the Fourier transform of the bare Coulomb potential with respect to the in-plane space dependence

$$v(\mathbf{r} - \mathbf{r}') = \frac{1}{A} \sum_{\mathbf{q}} e^{i\mathbf{q}(\mathbf{e} - \mathbf{e}')} v(\mathbf{q}, z - z'), \quad (\text{C4})$$

as well as the corresponding in-plane Fourier transform of the screened Coulomb interaction

$$w(\mathbf{e} - \mathbf{e}', z, z') = \frac{1}{A} \sum_{\mathbf{q}} e^{i\mathbf{q}(\mathbf{e} - \mathbf{e}')} w(\mathbf{q}, z, z'). \quad (\text{C5})$$

From Eq. (C1) an integral equation for the Fourier coefficients is readily obtained,

$$w(\mathbf{q}, z_1, z_2) = v(\mathbf{q}, z_1 - z_2) + \int dz_3 dz_4 v(\mathbf{q}, z_1 - z_3) P(\mathbf{q}, z_3, z_4) w(\mathbf{q}, z_4, z_2). \quad (\text{C6})$$

The interaction matrix elements for the bare Coulomb potential are given by Eq. (2) and similarly for the screened Coulomb potential. The assumed separation of wave functions into in-plane and  $z$  components allows us to introduce quasi-two-dimensional matrix elements. For the bare Coulomb interaction, the quasi-two-dimensional matrix elements are given by Eq. (4) where  $v(\mathbf{q}, z - z') = (e^2/2\epsilon_0 q) e^{-q|z - z'|}$  has been used. Then the interaction matrix elements follow from Eq. (5) or in the short notation

$$V_{\nu_1 \nu_2 \nu_3 \nu_4} = \frac{1}{A} \sum_{\mathbf{q}} V_{\sigma_1 \sigma_2 \sigma_3 \sigma_4}(\mathbf{q}) \langle \varphi_{\nu_1} | e^{-i\mathbf{q} \cdot \mathbf{e}} | \varphi_{\nu_4} \rangle \langle \varphi_{\nu_2} | e^{i\mathbf{q} \cdot \mathbf{e}} | \varphi_{\nu_3} \rangle, \quad (\text{C7})$$

where  $\sigma_i$  are the quantum numbers for the confinement in the  $z$  direction and the band indices  $b$  are suppressed for notational simplicity. For the screened Coulomb interaction we obtain in complete analogy

$$W_{\nu_1 \nu_2 \nu_3 \nu_4} = \frac{1}{A} \sum_{\mathbf{q}} W_{\sigma_1 \sigma_2 \sigma_3 \sigma_4}(\mathbf{q}) \langle \varphi_{\nu_1} | e^{-i\mathbf{q} \cdot \mathbf{e}} | \varphi_{\nu_4} \rangle \langle \varphi_{\nu_2} | e^{i\mathbf{q} \cdot \mathbf{e}} | \varphi_{\nu_3} \rangle, \quad (\text{C8})$$

where the corresponding in-plane matrix elements are given by

$$W_{\sigma_1 \sigma_2 \sigma_3 \sigma_4}(\mathbf{q}) = \int dz dz' \xi_{\sigma_1}^*(z) \xi_{\sigma_2}^*(z') w(\mathbf{q}, z_1, z_2) \xi_{\sigma_3}(z') \xi_{\sigma_4}(z). \quad (\text{C9})$$

The in-plane overlap integrals in the second line of Eq. (C8) have been discussed in Appendix B for the required combinations of WL and QD states. The remaining task is the computation of the in-plane matrix elements  $W_{\sigma_1 \sigma_2 \sigma_3 \sigma_4}(\mathbf{q})$ . Introducing in-plane matrix elements for the longitudinal polarization

$$P(\mathbf{q}, z_3, z_4) = \sum_{\sigma, \sigma'} \xi_{\sigma}(z) \xi_{\sigma'}(z') P_{\sigma, \sigma'}(\mathbf{q}) \xi_{\sigma}^*(z') \xi_{\sigma'}^*(z), \quad (\text{C10})$$

and using Eqs. (C9) as well as the corresponding equation for the bare Coulomb potential, the integral equation (C6)

can be reduced to the algebraic set of equations

$$W_{\sigma_1 \sigma_2 \sigma_3 \sigma_4}(\mathbf{q}) = V_{\sigma_1 \sigma_2 \sigma_3 \sigma_4}(\mathbf{q}) + \sum_{\sigma \sigma'} V_{\sigma_1 \sigma' \sigma \sigma_4}(\mathbf{q}) P_{\sigma \sigma'}(\mathbf{q}) W_{\sigma \sigma_2 \sigma_3 \sigma'}(\mathbf{q}). \quad (\text{C11})$$

A simple solution can be given if we assume identical confinement wave functions for the QD states  $\xi_O^*(z)$  to be distinguished from the  $z$  confinement in the WL,  $\xi_W^*(z)$ .

Finally we list the results for the Coulomb matrix elements used in Eqs. (6)–(10) to describe carrier capture and relaxation processes

$$W_{m_1 \mathbf{k}_2 \mathbf{k}_3 \mathbf{k}_4} = \frac{1}{A} W_{QWWW}(\mathbf{k}_2 - \mathbf{k}_3) \langle \varphi_{m_1} | e^{-i(\mathbf{k}_2 - \mathbf{k}_3) \cdot \mathbf{e}} | \varphi_{\mathbf{k}_4} \rangle F_{\mathbf{k}_2, \mathbf{k}_3}, \quad (\text{C12})$$

$$W_{m_1 \mathbf{k}_2 \mathbf{k}_3 m_4} = \frac{1}{A} W_{QWWQ}(\mathbf{k}_2 - \mathbf{k}_3) \langle \varphi_{m_1} | e^{-i(\mathbf{k}_2 - \mathbf{k}_3) \cdot \mathbf{e}} | \varphi_{m_4} \rangle F_{\mathbf{k}_2, \mathbf{k}_3}, \quad (\text{C13})$$

$$W_{m_1 \mathbf{k}_2 m_3 \mathbf{k}_4} = \frac{1}{A} \sum_{\mathbf{q}} W_{QWQW}(\mathbf{q}) \langle \varphi_{m_1} | e^{-i\mathbf{q} \cdot \mathbf{e}} | \varphi_{\mathbf{k}_4} \rangle \langle \varphi_{\mathbf{k}_2} | e^{i\mathbf{q} \cdot \mathbf{e}} | \varphi_{m_3} \rangle. \quad (\text{C14})$$

The in-plane Coulomb matrix elements are given by

$$W_{QWWW}(\mathbf{q}) = \frac{V_{QWWW}(\mathbf{q})}{1 - V_{WWW}(\mathbf{q}) P(\mathbf{q})}, \quad (\text{C15})$$

$$W_{QWWQ}(\mathbf{q}) = \frac{V_{QWWQ}(\mathbf{q})}{1 - V_{WWW}(\mathbf{q}) P(\mathbf{q})}, \quad (\text{C16})$$

$$W_{QWQW}(\mathbf{q}) = [V_{QWQW}(\mathbf{q}) - V_{QWQW}(\mathbf{q}) P(\mathbf{q}) V_{WWW}(\mathbf{q}) + V_{QWWW}(\mathbf{q}) P(\mathbf{q}) V_{WWQW}(\mathbf{q})] / [1 - V_{WWW}(\mathbf{q}) P(\mathbf{q})] \quad (\text{C17})$$

with  $P(\mathbf{q}) = P_{WW}(\mathbf{q})$ .

For the matrix elements  $W_{QWWW}$  and  $W_{QWWQ}$  it is directly possible to introduce a longitudinal dielectric function that obeys a generalized Lindhard formula when the longitudinal polarization is computed in random-phase approximation<sup>19</sup> for the OPW states

$$P(\mathbf{q}, \omega) = \frac{1}{A} \sum_{b, \mathbf{k}} \frac{f_{\mathbf{k}-\mathbf{q}}^b - f_{\mathbf{k}}^b}{\hbar \omega + \epsilon_{\mathbf{k}-\mathbf{q}}^b - \epsilon_{\mathbf{k}}^b + i\delta} |F_{\mathbf{k}, \mathbf{k}-\mathbf{q}}|^2, \quad (\text{C18})$$

where the frequency dependence has been added for completeness. The matrix structure of Eq. (C11) in principle prevents the simple structure with a generalized dielectric function for  $W_{QWQW}$  but the additional terms containing the polarization in the numerator of Eq. (C17) nearly compensate.

In conclusion, the assumed separation of the wave functions into in-plane and  $z$  components results in quasi-two-

dimensional matrix elements of the bare Coulomb interaction (4). Screening due to WL carriers can be included in this formula (for  $W_{m_1 k_2 k_3 k_4}$  and  $W_{m_1 k_2 k_3 m_4}$  strictly and for  $W_{m_1 k_2 m_3 k_4}$  in good approximation) by dividing with a longitudinal dielectric function  $\epsilon(\mathbf{q}, \omega) = 1 - V_{WWW}(\mathbf{q})P(\mathbf{q}, \omega)$  that contains the in-plane Coulomb interaction between WL states and their longitudinal polarization calculated with OPW corrections. For the presented calculations the generalized Lindhard formula is used in quasistatic approximation.

#### APPENDIX D: ROLE OF THE WAVE-FUNCTION MODEL

In this appendix we discuss the influence of various assumptions of the wave-function model on the calculated scattering rates. In lens-shaped QD's on a WL the spatial height of the  $z$  confinement changes within the QD. In the adiabatic approximation discussed in Ref. 17 the wave function contains in-plane and  $z$ -confinement parts according to

$$\Phi_\nu(\mathbf{r}) = \varphi_i^b(\boldsymbol{\rho}) \xi_\sigma^b(\boldsymbol{\rho}, z) u_b(\mathbf{r}). \quad (\text{D1})$$

For a confinement potential with cylindrical symmetry, the in-plane part can be expressed using  $\varphi_i^b(\boldsymbol{\rho}) = e^{im\phi} / \sqrt{2\pi} f_i(\rho)$  with the in-plane angle  $\phi$ . For a discretization of the potential into ring-shaped regions of (approximately) constant  $z$  confinement  $f_i(\rho)$  obeys Bessel's differential equation. Boundary conditions determine the matching of wave functions in different regions. This procedure allows us to construct piecewise analytically determined wave functions for a given confinement geometry. Nevertheless, using these wave functions in Eq. (5) is a challenging task since for an appropriate discretisation of the WL continuum a large number of Coulomb matrix elements is required.

Instead of using this approach we checked on a simpler level, how sensitive the discussed calculations of scattering rates are to the particular choice of confinement wave functions. We consider two limiting cases.

(i) Constant height  $z_{\text{QD}}$  within the QD and smaller height  $z_{\text{WL}}$  throughout the WL. (For shallow QD's the wave functions average over a weakly changing height.)

(ii) In the limit of equal  $z$  confinement for QD and WL the QD confinement would be purely due to composition changes and/or strain in the  $x$ - $y$  plane.

In both cases, Eq. (D1) reduces to Eq. (3). In the first case of different confinement functions  $\xi_\sigma^b(z)$  for the QD and WL states, a three-dimensional OPW scheme according to

$$|\Phi_{\mathbf{k}}\rangle = \frac{1}{N_{\mathbf{k}}} \left( |\Phi_{\mathbf{k}}^0\rangle - \sum_{\alpha} |\Phi_{\alpha}\rangle \langle \Phi_{\alpha} | \Phi_{\mathbf{k}}^0 \rangle \right) \quad (\text{D2})$$

is necessary. We compared results for the QD relaxation rates  $S^{1\text{D}}$  based on this scheme (solid line in Fig. 9) with a simplified calculation where only the in-plane part of the wave functions  $\varphi_i^b(\boldsymbol{\rho})$  is subject to the OPW scheme according to Eq. (A1) and different  $z$ -confinement functions enter in the form factor of the in-plane Coulomb-matrix elements, Eq. (4). Both in- and out-scattering rates of electrons and holes are practically unchanged and differences would not be visible in Fig. 9.

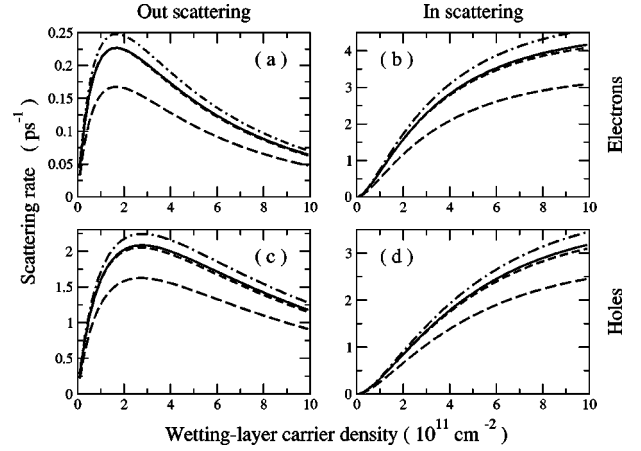


FIG. 9. Scattering rates for QD carrier relaxation processes  $S^{1\text{D}}$  similar to Fig. 4 but with different approximations for the confinement wave functions. Solid line: OPW calculation, short-dashed line: plane-wave WL states, long-dashed line: larger QD height and smaller WL thickness, dashed-dotted line: equal confinement in growth direction for QD and WL.

The result using plane waves for the in-plane part of the WL states is shown as short-dashed line in Fig. 9. For the relaxation rates  $S^{1\text{D}}$  the Coulomb interaction matrix elements contain only pairing of WL states or pairing of QD states. Hence the missing orthogonality of plane waves and QD states does not influence the results and OPW corrections are small. The situation is different for the carrier capture rates where Coulomb interaction matrix elements contain pairings of WL and QD states. For the capture rates to the first excited states, Fig. 10, the plane-wave results (short-dashed lines) strongly depart from the OPW calculations. On the other hand, deviations between 3D-OPW results (solid lines) and the 2D-OPW model (dotted lines) are small. Similar results (not shown) are found for the scattering rates  $S^{2\text{D}}$ ,  $S^{12\text{X}}$  and  $S^{\text{mixed}}$ . Since the 2D-OPW model greatly simplifies the calculations, it has been used in Figs. 3–8.

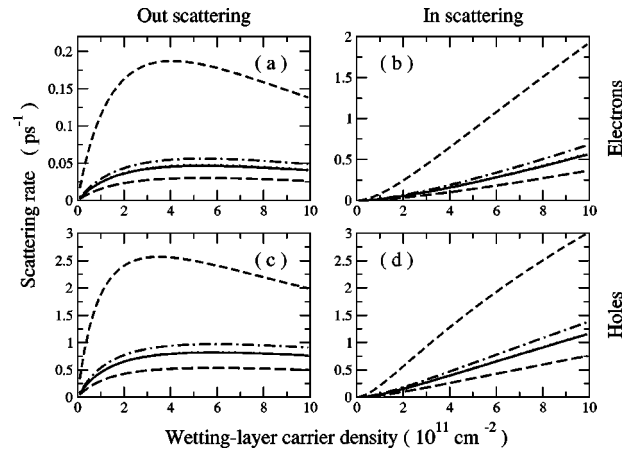


FIG. 10. Scattering rates for carrier capture from WL to first excited QD states similar to Fig. 3 but with different approximations for the confinement wave functions. Solid line: 3D-OPW calculation, dotted line: 2D-OPW model. For other lines, see Fig. 9.

Next we investigate the dependence of the results on the particular choice of parameters for the confinement potential. While variations of the confinement potential will also affect the QD energies, we are here only interested in the influence of the confinement potential on the Coulomb matrix elements. Hence, we artificially use the same QD energies as before but take different functions  $\xi_{\sigma}^b(z)$ . While previous calculations are done for 2.2 nm WL height and additional 2.1 nm QD height, the long-dashed lines in Figs. 9 and 10 correspond to a 1.6 nm WL height and additional 4.4 nm QD height (using the 2D-OPW model). While this is a rather

large change of the confinement situation, the changes of the scattering rates are relatively small. The dashed-dotted lines in Figs. 9 and 10 show results for the limiting case of equal confinement in the  $z$  direction for QW and WL discussed above. Calculations are done for a 4 nm finite-height confinement potential. Due to the maximized overlap for the  $z$  components of the QD and WL wave functions, the scattering rates are larger than in the previous cases. The capture and relaxation times for this situation using GaAs parameters are given in Ref. 20.

---

\*Corresponding author: e-mail: jahnke@physik.uni-bremen.de

<sup>1</sup>P. Bhattacharya, K. K. Kamath, J. Singh, D. Koltzkin, J. Phillips, H.-T. Jiang, N. Chervela, T. B. Norris, T. Sosnowski, J. Laskar, and M. R. Murty, IEEE Trans. Electron Devices **46**, 871 (1999).

<sup>2</sup>G. Park, O. B. Shchekin, D. L. Huffaker, and D. G. Deppe, Electron. Lett. **36**, 1283 (2000).

<sup>3</sup>P. Borri, W. Langbein, J. M. Hvam, F. Heinrichsdorff, M.-H. Mao, and D. Bimberg, IEEE Photonics Technol. Lett. **12**, 594 (2000).

<sup>4</sup>J. Zimmermann, S. T. Cundiff, G. von Plessen, J. Feldmann, M. Arzberger, G. Böhm, M.-C. Amann, and G. Abstreiter, Appl. Phys. Lett. **79**, 18 (2001).

<sup>5</sup>W. W. Chow and S. W. Koch, *Semiconductor-Laser Fundamentals* (Springer, Berlin, 1999).

<sup>6</sup>U. Bockelmann and T. Egeler, Phys. Rev. B **46**, 15 574 (1992).

<sup>7</sup>A. V. Uskov, F. Adler, H. Schweizer, and M. H. Pilkuhn, J. Appl. Phys. **81**, 7895 (1997).

<sup>8</sup>R. Ferreira and G. Bastard, Appl. Phys. Lett. **74**, 2818 (1999).

<sup>9</sup>M. Braskén, M. Lindberg, and J. Tulkki, Phys. Status Solidi A **164**, 427 (1997).

<sup>10</sup>I. Magnusdottir, S. Bischoff, A. V. Uskov, and J. Mørk, Phys.

Rev. B **67**, 205326 (2003).

<sup>11</sup>T. Inoshita and H. Sakaki Phys. Rev. B **46**, 7260 (1992).

<sup>12</sup>H. Jiang and J. Singh, IEEE J. Quantum Electron. **34**, 1188 (1998).

<sup>13</sup>B. Ohnesorge, M. Albrecht, J. Oshinowo, A. Forchel, and Y. Arakawa, Phys. Rev. B **54**, 11 532 (1996).

<sup>14</sup>D. Morris, N. Perret, and S. Fafard, Appl. Phys. Lett. **75**, 3593 (1999).

<sup>15</sup>S. Raymond, K. Hinzer, S. Fafard, and J. L. Merz, Phys. Rev. B **61**, R16331 (2000).

<sup>16</sup>S. Sanguinetti, K. Watanabe, T. Tateno, M. Wakaki, N. Koguchi, T. Kuroda, F. Minami, and M. Gurioli, Appl. Phys. Lett. **81**, 613 (2002).

<sup>17</sup>A. Wojs, P. Hawrylak, S. Fafard, and L. Jacak, Phys. Rev. B **54**, 5604 (1996).

<sup>18</sup>H. C. Schneider, W. W. Chow, and S. W. Koch, Phys. Rev. B **64**, 115315 (2001).

<sup>19</sup>G. D. Mahan, *Many-Particle Physics* (Plenum, New York, 1990).

<sup>20</sup>T. Nielsen, P. Gartner, and F. Jahnke, Phys. Status Solidi C **0**, 1532 (2003).